

Structural and Spectroscopic Studies of the Copper Site of Stellacyanin<sup>†</sup>Richard W. Strange,<sup>‡</sup> Bengt Reinhammar,<sup>§</sup> Loretta M. Murphy,<sup>‡</sup> and S. Samar Hasnain<sup>\*‡</sup>*Molecular Biophysics Group, Daresbury Laboratory, Warrington WA4 4AD, Cheshire, U.K., and Department of Biochemistry and Biophysics, Chalmers University of Technology and Göteborg University, Göteborg, Sweden**Received July 25, 1994; Revised Manuscript Received November 1, 1994<sup>®</sup>*

**ABSTRACT:** The structure of the copper site in oxidized and reduced *Rhus vernicifera* stellacyanin has been studied by X-ray absorption (XAFS) spectroscopy at different pH values. Data for the oxidized protein are consistent with the fourth ligand being an O- or N-donating ligand rather than a cysteine from the disulfide bridge. The fourth ligand is not present in the inner coordination sphere, but makes a more distant interaction 2.7 Å from the copper atom. Only minor changes in the details of the Cu(II) coordination occur when the pH is varied. Direct structural information on reduced stellacyanin is provided. Upon reduction, one of the histidine ligands moves away from the copper atom by at least 0.2 Å. A low-Z (O or N) scatterer is present ~2.4 Å from the Cu(I) atom in the protein at low pH, and this ligand is lost at high pH. There is no evidence for an S-donating fourth ligand in the reduced protein. The XAFS results are presented in relation to the spectroscopic and structural information available for some methionine-121 mutants of azurin. The data reveal that there are spectroscopic similarities between stellacyanin and some of the mutant proteins, but distinct structural differences exist that preclude these proteins as suitable models for the copper site of stellacyanin.

Stellacyanin is a type 1 (blue) single-copper protein isolated from the sap of the Japanese lacquer tree *Rhus vernicifera* (Reinhammar, 1970). Unlike azurin, plastocyanin, and cucumber basic protein (CBP), for which high-resolution crystallographic data are available (Adman & Jensen, 1981; Norris et al., 1986; Baker, 1988; Guss & Freeman, 1983; Guss et al., 1988; Fields et al., 1991), stellacyanin so far has resisted crystallization attempts. However, from a number of spectroscopic studies, such as Raman spectroscopy (Blair et al., 1985), ENDOR (Roberts et al., 1984; Thomann et al., 1991), EXAFS (Peisach et al., 1982; Feiters et al., 1988), and NMR (Hill & Lee, 1979), as well as sequence homology with azurin, plastocyanin, and CBP (Bergman et al., 1977; Guss et al., 1988), the copper atom in stellacyanin is known to share the same basic Cu(II) coordination common to the other type 1 copper proteins. On the other hand, there is little data currently available on the structure of the copper site in reduced stellacyanin.

The typical type 1 Cu(II) site consists of an inner coordination sphere of two histidine ligands and a cysteine ligand. In azurin, plastocyanin, and CBP, a fourth, more distant ligand, is supplied by a sulfur from a methionine residue. However, stellacyanin does not possess any methionine residues (Bergman et al., 1977), and the identity of a fourth ligand to Cu has been the subject of much discussion. Three cysteine residues (Cys59, Cys87, and Cys93) are known to be present in stellacyanin. One of these residues is a ligand to Cu, akin to the cysteine ligand in other blue proteins, while the other two residues are believed to form a disulfide bridge (Bergman et al., 1977; Engeseth et al., 1984). It should be noted that CBP has three cysteine residues homologous with stellacyanin, Cys52, Cys79, and

Cys85. There is a disulfide bridge between Cys52 and Cys85, and Cys79 is the copper ligand (Guss et al., 1988). There is some spectroscopic evidence that the three S(Cys) atoms in stellacyanin are all close to the copper site, and it has been suggested, by analogy with azurin and plastocyanin, that the fourth ligand in stellacyanin is provided by one of the S atoms of the disulfide bridge (Bergman et al., 1977; McMillin & Morris, 1981; Ferris et al., 1978; Solomon et al., 1980; Feiters et al., 1988; Dahlin et al., 1989). Molecular modeling studies based on the sequence homology between stellacyanin and poplar plastocyanin have supported this possibility (Wherland et al., 1988), as has a <sup>1</sup>H NMR study on Co(II) stellacyanin (Dahlin et al., 1989). On the other hand, a molecular modeling study based on the sequence homology between stellacyanin and CBP suggests that the fourth ligand in stellacyanin is a glutamine residue, Gln97 (Guss et al., 1988; Fields et al., 1991). This proposal has received support from ENDOR studies, which showed evidence for nitrogen as the fourth ligand in the high-pH form of stellacyanin. At low pH the nitrogen resonance is not present. The fourth ligand therefore exhibits pH dependence consistent with copper amide chemistry, in which the carbonyl oxygen may be the coordinating group at low pH, with the amide group nitrogen coordinated at high pH (Thomann et al., 1991).

There is considerable general interest in how the same basic framework of histidine and cysteine ligands, found for all structurally characterized small blue proteins, is fine tuned to give redox potentials ranging from 184 mV for stellacyanin to 680 mV for rusticyanin from *Thiobacillus ferrooxidans* (Reinhammar, 1979; Adman, 1985). In particular, the role of methionine (or another fourth ligand) has been discussed extensively in terms of a fine tuning mechanism (Gray & Malmström, 1983; Guss et al., 1986). In this paper, we use X-ray absorption fine structure (EXAFS) to examine the copper center of stellacyanin directly. Previous EXAFS studies (Peisach et al., 1982; Feiters et al., 1988) have not

<sup>†</sup> This research was supported by the Science and Engineering Research Council (U.K.) and the Swedish Research Council.

<sup>‡</sup> Daresbury Laboratory.

<sup>§</sup> Chalmers University of Technology and Göteborg University.

<sup>®</sup> Abstract published in *Advance ACS Abstracts*, December 1, 1994.

unambiguously determined the presence of a second sulfur ligand to stellacyanin. We apply curved-wave multiple-scattering EXAFS theory, combined with a constrained/restrained refinement method (Binsted et al., 1992), to study the EXAFS of oxidized and reduced stellacyanin at two pH values, 6.4 and 11.0. These pH values span the range in which reversible changes in the optical absorption and EPR spectra have been observed (Malmström et al., 1970). The Cu(II) EXAFS is discussed in relation to the spectrochemical properties of the protein, including its optical and electron paramagnetic resonance (EPR) data. The spectroscopic and structural properties of Cu(II) stellacyanin are also discussed in relation to other type 1 copper proteins, in particular azurins from both *Pseudomonas aeruginosa*, in which site-directed mutagenesis has been used to replace (or delete) the methionine ligand (Karlsson et al., 1991), and *Alcaligenes denitrificans*, in which an X-ray structure has recently been obtained for a mutant wherein the methionine residue has been replaced by glutamine (Romero et al., 1993). The copper site in this mutant has been proposed as a model for the copper site of stellacyanin, with the glutamine ligand coordinated to Cu(II) at 2.26 Å. We also consider the possibility that a second cysteine provides a ligand to the Cu(II) atom, analogous to the role played by methionine in other type 1 Cu proteins. For the reduced protein, where a comparison with spectroscopic data is not feasible, we present possible models of the structure of the Cu(I) site based upon the EXAFS results for the first time. We consider these results in relation to the crystal structure of the Cu(I) form of the glutamine mutant of *A. denitrificans* azurin (Romero et al., 1993), which shows one of the copper-histidine distances to be increased by about 1 Å compared to the oxidized form.

## MATERIALS AND METHODS

**Materials.** All chemicals were reagent grade and used without further purification. Water was deionized using a Elgastat water treatment system. All final stage concentrations were performed using Centricon-10 concentrators for the oxidized samples and a Model 3 stirred cell, pressurized with ultrapure argon, for the reduced samples (both types of concentrator were from Amicon Ltd., Upper Mill, U.K.).

**Preparation of Stellacyanin Samples.** *Rhus vernicifera* stellacyanin was prepared (Reinhammar, 1970) from an acetone fraction of Japanese lacquer (obtained from Saito & Co. Ltd). The protein was stored as a lyophilized powder at -20 °C until required. Stellacyanin (80 mg) was dissolved in 0.5 mL of water; one half was dialyzed versus 50 mM sodium acetate buffer (pH 6.4), and the other half was dialyzed versus 50 mM sodium borate buffer (pH 11.0). The X-band EPR and optical spectra of the samples were recorded after dialysis. Approximately half of each protein solution, at both pH values, was then removed for subsequent reduction. The remaining oxidized samples were concentrated to a volume of ca. 400 µL each. Reduction of the protein samples was performed by placing each sample in an Amicon stirred concentration cell. Pressurized with ultrapure argon, in approximately 2 mL of the appropriate buffer. The volume was reduced to 400 µL, and then a small aliquot (10 µL) of 1 M sodium ascorbate dissolved in degassed buffer was added. Bleaching of the intense blue color of the samples was taken as a visual indication of reduction. The samples were frozen in liquid nitrogen.

**X-ray Absorption Spectroscopy.** Copper K-edge extended X-ray absorption fine structure (EXAFS) measurements were carried out in the fluorescence mode at the Synchrotron Radiation Source at the Daresbury Laboratory on Wiggler beam line 9.2. The synchrotron was operating at 2 GeV with an average beam current of 160 mA. A Si(220) double crystal, order-sorting monochromator was used to minimize the harmonic content of the monochromatic beam. A 13-element Ge solid-state detector was used to record the fluorescence data. The protein samples were placed in Perspex sample cells with Mylar windows and frozen in liquid nitrogen. The sample cell window dimensions were 8 × 10 × 2 mm (height × width × depth). The protein samples were measured as frozen solutions at ca. 77 K in a liquid nitrogen cryostat. Data were obtained for four samples: two oxidized Cu(II) samples at pH 6.4 (ox6.4) and pH 11.0 (ox11.0), and two reduced Cu(I) samples at pH 6.4 (red6.4) and pH 11.0 (red11.0). For EXAFS data collection, a beam size of 3 × 5 mm (height × length) was used; this was reduced to a height of 0.75 mm for X-ray absorption near-edge structure (XANES) data collection. The X-ray energy was calibrated by scanning a 5 µm Cu foil in the transmission mode and setting the first inflection point on the absorption edge equal to 8982 eV. An average of 12 scans per sample was recorded. After the output of each detector element was checked individually for glitches or anomalies in the data, the scans were averaged. After calibration of the monochromator angle to energy, the EXAFS was normalized to a unit Cu atom and extracted from the background absorption using the Daresbury Laboratory program EXBACK (Morrell et al., 1989). The EXAFS data were converted into *k*-space using  $k = [2m_e(E - E_0)/h^2]^{1/2}$ , where *E* and *E*<sub>0</sub> are the energies of the incident X-ray radiation and the absorption edge of the Cu atom, respectively, and *k* is the photoelectron wave vector.

Analysis of the EXAFS data was performed using the nonlinear least-squares program EXCURV92 (Binsted et al., 1991), which calculates the theoretical EXAFS function using fast curved-wave theory and incorporates multiple scattering up to third order (Gurman et al., 1984, 1986). Curve fitting was carried out in *k*-space on raw EXAFS data weighted by *k*<sup>3</sup> to compensate for the diminishing amplitude of the EXAFS at high *k*. The quality of the simulations was assessed by the following: (i) the least-squares fit index (FI), which is defined as  $FI = \sum_i |k^3(\chi^{exp}(k_i) - \chi^{th}(k_i))|^2/n^2$ , where  $n = \sum_i k^3|\chi^{exp}(k_i)|$ , and  $\chi^{exp}(k_i)$  and  $\chi^{th}(k_i)$  are the experimental and theoretical EXAFS, respectively, (ii) an *R*-factor, *R*<sub>ε</sub>, which is given by  $R_\epsilon = \sum_i k^3|(\chi^{exp}(k_i) - \chi^{th}(k_i))|/n \times 100$ , (iii) an *R*-factor, *R*<sub>d</sub>, where  $R_d = \sum_i 1/\sigma_i |(r_i^{ref} - r_i^{ideal})|/r_i^{ideal} \times 100$ , where  $1/\sigma_i = (1/\sigma_i^{dist})/(\sum_j 1/\sigma_j^{dist})$  is the weighting factor applied to an ideal crystallographic distance *r*<sup>ideal</sup>, and *r*<sup>ref</sup> is the distance obtained by least-squares refinement. The value of *R*<sub>d</sub> gives the percent mean error in bond distance from the ideal crystallographic value taken from small molecule X-ray structures. For imidazole ring interatom distances, we have chosen a cutoff value of *R*<sub>d</sub> ≤ 1%. The relative significance of the EXAFS and ideal distance refinements is determined by weighting their contributions to the final fit. In all calculations, unless otherwise stated, we have used weightings of 0.5 (EXAFS refinement) and 0.5 (distance refinement). The procedure is described in detail in Binsted et al. (1992).

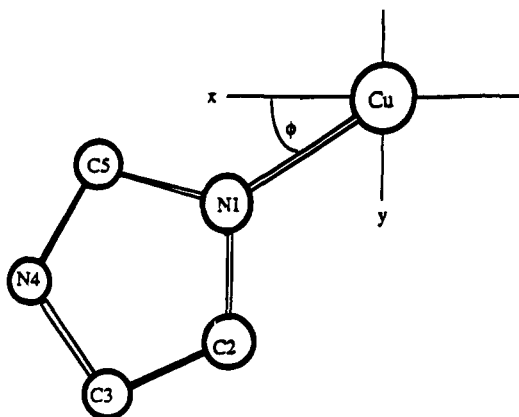


FIGURE 1: Imidazole ring geometry showing numbering scheme used in the text. Atomic positions are described by polar coordinates  $r$ ,  $\phi$ , and  $\theta$ , where  $\theta = 90^\circ$  is the  $x,y$  plane.

Finally, a simulation was assessed by visual inspection of the fitted data for both EXAFS and Fourier transforms. The phase shifts employed in the data analysis were calculated *ab initio* using the program MUFPO. The Cu, N, C, and O phase shifts have previously been used to simulate a number of Cu-histidine and Cu-pyridine model compounds (Strange et al., 1987; Blackburn et al., 1988), as well as the Cu site of superoxide dismutase (Blackburn et al., 1987). Full curved-wave, multiple-scattering analysis was included in the preceding cases. The central atom (copper) phase shifts employed here were calculated assuming a neutral  $Z+1$   $1s$  core hole excited state. This approximation was also used for analysis of the XAFS of a number of methionine-121 azurin mutants (Murphy et al., 1993). However, a different central atom approximation was used by Feiters et al. (1988), who used a double positive charge on the copper atom. As will be seen, this leads to some differences in interpretation of the EXAFS data. The photoelectron energy threshold,  $E_0$ , was treated as a single overall parameter for the multiple shell fits.

Constrained and restrained refinement procedures were used to minimize the number of free parameters in the least-squares refinement (Hasnain & Strange, 1990; Binsted et al., 1992). In the constrained refinement method, the imidazole ring associated with the histidine ligand is treated as a single rigid unit with a well-defined ideal geometry. The parameters used to construct this unit are taken from the averaged bond distances and angles of nearly 200 crystallographically characterized Cu-imidazole model compounds (Orpen et al., 1989). Both histidine ligands were initially assumed to be coordinating at the same distance to Cu; therefore, the EXAFS due to a single imidazole unit so defined, including its multiple-scattering contribution, was doubled during refinement. This method results in a significant reduction in the number of independent parameters during refinement. Since the contributions of the ring atoms are spatially fixed, backscattering atoms external to the ring are more easily distinguished and can be picked out with more confidence.

To further reduce the number of refinable parameters, the Debye-Waller factors ( $\alpha = 2\sigma^2$ ) of the C2/C5 and C3/N4 atoms of the imidazole ring (Figure 1) were refined together as a single variable. A further constraint was that refinement should be limited to a situation where  $\alpha(1) < \alpha(2,5) < \alpha(3,4)$ ; it is physically unrealistic to allow the more distant atoms of a ring structure to have a stronger thermal

correlation with the metal atom than the nearest neighbor atoms of the ring. This results in a total of nine independent parameters for the basic constrained model. Six of these parameters are derived from the imidazole ring— $R1$ ,  $\alpha(1)$ ,  $\alpha(2,5)$ , and  $\alpha(3,4)$ , plus one  $\theta$  parameter and  $\phi$  parameter; two parameters are from the S(Cys) shell,  $R6$  and  $\sigma(6)$ , plus the  $E_0$  parameter. For restrained refinement, the number of parameters is increased to 12 for the five atoms of an imidazole ring—this includes  $R(1-5)$ ,  $\phi(2-5)$ , and the three Debye-Waller parameters. The fitting procedure consisted of successive cycles of constrained refinement followed by restrained refinement, as described in Hasnain and Strange (1990) and Binsted et al. (1992). The  $\theta$  parameters were kept fixed during restrained refinement. For the oxidized stellacyanin data, where the two histidine rings were found to be coordinated at the same distance, the total number of independent parameters was 16–18. For the reduced EXAFS data it was necessary to try models that included the two histidines at different distances (separated by  $\sim 0.2$  Å). In this case, the total number of independent parameters was about 30. The additional observations introduced by the restrained refinement method meant that in this case the refinement was only just determined (Binsted et al., 1992).

## RESULTS

**Absorption Edges and Near-Edge Structure.** Figure 2 shows the normalized absorption edge data for the oxidized and reduced forms of stellacyanin at pH 6.4 and 11.0. The oxidized spectra are virtually identical and have a low-energy (8979 eV) feature (marked *a*) typically associated with the Cu(II) oxidation state. The edges for the reduced protein exhibit a rising shoulder at 8983–8986 eV. This region has been associated with transitions from the Cu  $1s$  core state to the  $4p_z$  and  $4p_{xy}$  final states (Kau et al., 1987). The intensity (and sharpness) of the 8983 eV peak in Cu(I) (marked *b*) has been shown to correlate with the degree of displacement of the copper atom from the ligand plane (Blackburn et al., 1989). In particular, the amplitude of this peak decreases as the structure goes from a linear two-coordinate or three-coordinate geometry toward trigonal-pyramidal, pseudotetrahedral, or tetrahedral geometry. In the light of these studies, the edge spectra in Figure 2 suggest that at both pH 6.4 and 11.0 the Cu site in reduced stellacyanin is three-coordinate (or more), but with a significantly distorted trigonal geometry.

Included for comparison in Figure 2 are the reversible pH dependent optical and EPR data for oxidized stellacyanin. The visible spectrum at pH 7.0 shows strong absorption bands at 450 and 604 nm, which are shifted by about 20 nm to higher energy at pH 11.0, suggesting increased charge transfer to the copper. The X-band EPR spectra at 77 K show type 1 Cu(II) character at both pH values, although the parameters change significantly with pH (Malmström et al., 1970).

**EXAFS Data Analysis.** The  $k^3$ -weighted raw EXAFS spectra of oxidized Cu(II) and reduced Cu(I) stellacyanin at pH 6.4 and 11.0 are shown in Figure 3. In each case, the basic coordination to the copper atom is expected to consist of two histidine ligands and a cysteine ligand. These ligands provide the predominant contribution to the EXAFS and explain the close similarity between the two Cu(II) spectra. The phase-corrected Fourier transforms corresponding to the

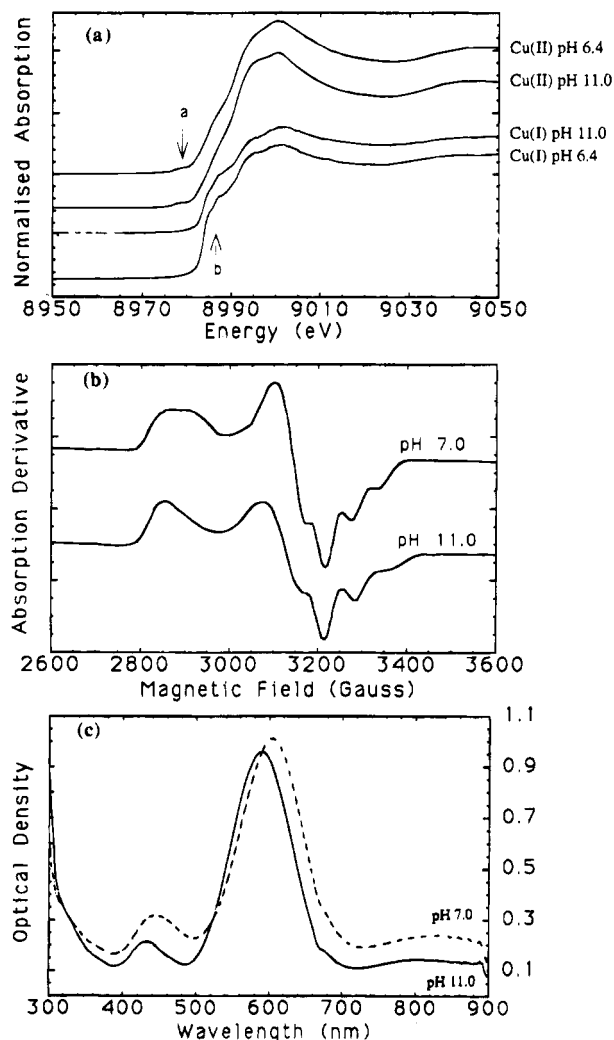


FIGURE 2: (a) Normalized copper X-ray absorption K-edges for oxidized and reduced forms of stellacyanin at pH 6.4 and 11.0. Absorption features typically associated with Cu(II) and Cu(I) K-edges at  $\sim 8979$  (marked a) and  $\sim 8985$  eV (marked b) are indicated. (b) EPR spectra for stellacyanin at pH 7.0 and 11.0. (c) Optical absorption spectra for stellacyanin at pH 7.0 and 11.0.

EXAFS data are shown in the lower panel of Figure 3. The Fourier transforms show that there are three main shells of atoms contributing to the EXAFS, at distances of ca. 2, 3.0, and 4.0–4.5 Å. The Cu–N(His) and Cu–S(Cys) backscattering contributions are expected to be present in the first of these shells. The second and third shells in the Fourier transform are primarily due to backscattering from the second- and third-shell atoms of the imidazole rings of the two histidine ligands. Multiple scattering is expected to contribute from these atoms (Strange et al., 1987). There may also be additional contributions from other atoms in this region. Inspection of Figure 3 shows that differences exist between each of the spectra. More specifically, for the oxidized protein the differences are most pronounced in the first two beat regions, between  $k = 4.0\text{--}5.6$  Å $^{-1}$  and  $k = 5.6\text{--}8.0$  Å $^{-1}$ . These differences suggest a subtle variation in the Cu coordination upon altering the pH. By contrast, upon reduction of the copper, the EXAFS profile displays an overall higher frequency, indicating a lengthening of the primary distance. The Fourier transforms also display this effect, with the primary distance increasing as ox6.4 < ox11.0 < red11.0 < red6.4. In the case of the reduced protein, the Fourier transforms depict relatively weaker

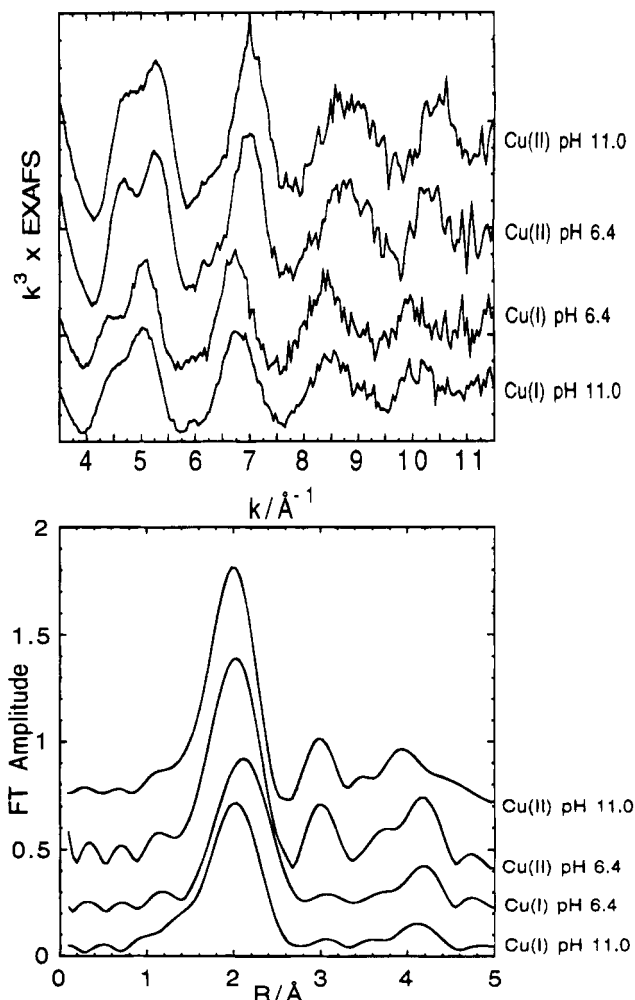


FIGURE 3:  $k^3$ -weighted raw EXAFS data and corresponding Fourier transforms for oxidized and reduced stellacyanin at pH 6.4 and 11.0.

contributions in the 3–4 Å region, indicating either a significant movement or the loss of a histidine ligand from the primary shell. This observation is supported by the decreased amplitude of the peak at ca. 2 Å compared with the oxidized data.

**Analysis of Oxidized Stellacyanin.** The model initially adopted for data analysis was the basic one common to the blue copper proteins, such as azurin and plastocyanin, that have been characterized extensively by X-ray crystallography and EXAFS. This model consists of an inner Cu(II) coordination sphere of two histidine ligands and a cysteine ligand. The methionine ligand, present in both the azurin and plastocyanin families, is absent from stellacyanin; a second sulfur ligand therefore was excluded from the initial model. A carbonyl group from a glycine ligand, present in the azurin crystal structure at ca. 3.0 Å, was also excluded from the initial analysis.

**(1) ox11.0 EXAFS.** The major contribution to the EXAFS of the oxidized protein at pH 11.0 was accounted for by a simulation using a basic model of two histidine ligands at 1.89 Å and one S(cysteine) ligand at 2.13 Å. However, the theory gave inadequate intensity in the second shell ( $\sim 3$  Å) of the Fourier transform compared with experiment (FI = 0.098,  $R_d = 0.48\%$ ,  $R_e = 21.6\%$ ). Previous spectroscopic and structural studies on stellacyanin suggest two possible candidates for a shell at  $\sim 3$  Å: either a nitrogen/oxygen ligand (Thomann et al., 1991) or a sulfur ligand (Bergman

Table 1: Parameters Used in the Simulations of Oxidized Stellacyanin at pH 11.0<sup>a</sup>

	<i>R</i> (Å)	2σ <sup>2</sup> (Å <sup>2</sup> )	φ (deg)	θ (deg)
2N(His)	1.89	0.004	0.0	90.0
2C(His)	2.90	0.007	339.6	91.6
2C(His)	2.85	0.007	24.2	91.4
2N(His)	3.99	0.019	352.3	92.9
2C(His)	4.01	0.019	12.2	92.9
1S(Cys)	2.13	0.001		
1N <sup>b</sup> (1S <sup>c</sup> )	2.69 (2.91)	0.007 (0.025)		

<sup>a</sup> The distance (*R*) and Debye–Waller term (2σ<sup>2</sup>) for each shell are shown together with the polar angles (φ, θ) of the imidazole ring atoms, as defined in Figure 1. <sup>b</sup> Nitrogen at 2.69 Å (FI = 0.071, *R*<sub>d</sub> = 0.51%, *R*<sub>e</sub> = 17.3%) and <sup>c</sup>sulfur at 2.91 Å (FI = 0.079, *R*<sub>d</sub> = 0.47%, *R*<sub>e</sub> = 18.4%) are alternative models (see text).

Table 2: Parameters Used in the Simulations of Oxidized Stellacyanin at pH 6.4<sup>a</sup>

	<i>R</i> (Å)	2σ <sup>2</sup> (Å <sup>2</sup> )	φ (deg)	θ (deg)
<sup>b</sup> 2N(His)	1.90	0.004	0.0	90.0
2C(His)	2.93	0.007	339.7	90.8
2C(His)	2.89	0.007	23.9	90.7
2N(His)	4.02	0.019	352.2	91.4
2C(His)	4.03	0.019	11.8	91.4
1S(Cys)	2.14	0.002		
1O	2.70	0.005		
1S	4.34	0.010		
<sup>c</sup> 2N(His)	1.90	0.004	0.0	90.0
2C(His)	2.95	0.014	339.7	90.8
2C(His)	2.88	0.014	23.9	90.7
2N(His)	4.02	0.021	352.2	91.4
2C(His)	4.03	0.021	11.8	91.4
1S(Cys)	2.14	0.002		
1S	3.00	0.024		
1S	4.34	0.010		

<sup>a</sup> The distance (*R*) and Debye–Waller term (2σ<sup>2</sup>) for each shell are shown together with the polar angles (φ, θ) of the imidazole ring atoms, as defined in Figure 1. <sup>b</sup> The parameters with oxygen at 2.70 Å (FI = 0.078, *R*<sub>d</sub> = 0.88%, *R*<sub>e</sub> = 16.9%) and sulfur at 4.34 Å (FI = 0.065, *R*<sub>d</sub> = 0.88%, *R*<sub>e</sub> = 15.3%). <sup>c</sup> Alternative parameters using sulfur at 3.0 Å instead of oxygen (FI = 0.081, *R*<sub>d</sub> = 1.0%, *R*<sub>e</sub> = 17.9%).

et al., 1977; McMillin & Morris, 1981; Ferris et al., 1978; Solomon et al., 1980; Dahlin et al., 1989). Simulations based upon both of these possibilities were attempted. A simulation based on a sulfur ligand at ~2.9 Å produced an anomalously high α of 0.025 Å<sup>2</sup> (Table 1). A simulation using a weaker contributor, nitrogen, at ~2.7 Å resulted in a much improved fit, with α = 0.007 Å<sup>2</sup> (Table 1 and Figure 4).

(2) *ox6.4 EXAFS*. A simulation of the EXAFS of the oxidized data at pH 6.4 also showed that an additional shell at ~3 Å was required to fit the data. Inclusion of an oxygen atom at 2.7 Å (α = 0.005 Å<sup>2</sup>) in addition to the two histidines and one S(Cys), produced a simulation with FI = 0.078 (Figure 5a). The Fourier transforms suggest that there is a contribution to the EXAFS at ~4.3 Å that remains unaccounted for by this model. This could be improved in two ways: in the first case, a single sulfur atom could be added at ~4.3 Å (α = 0.010 Å<sup>2</sup>), which leads to a 13% decrease in FI (Figure 5b). Alternatively, the outer shell fit could be improved by adding two shells of low-Z atoms (carbons): 3C at ~4.2 Å and 3C at ~4.6 Å. There is one additional shell in the latter model compared to the model using a single sulfur at ~4.3 Å. The Debye–Waller parameters for the outer shell atoms of the imidazole rings are increased from 0.014 to 0.019 Å<sup>2</sup> when either the sulfur or carbon atom is present. (We note that inclusion of either sulfur or carbon

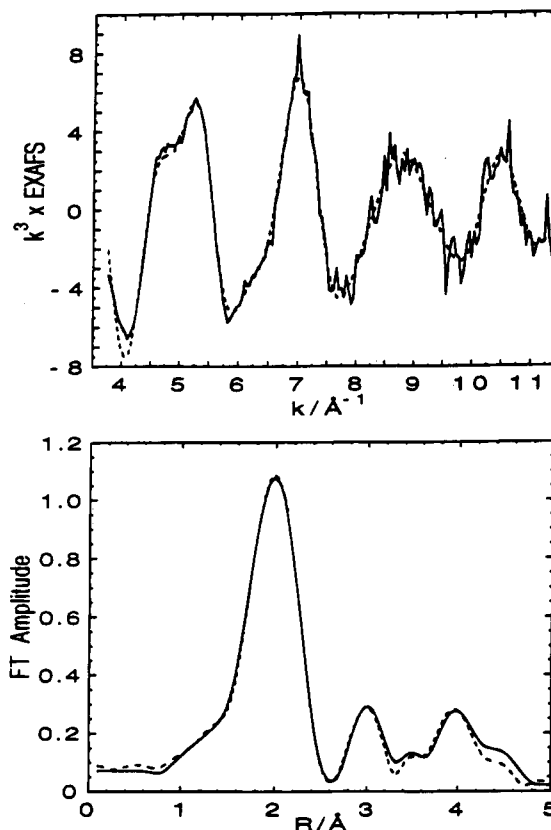


FIGURE 4: Simulation (dashed line) of oxidized stellacyanin EXAFS at pH 11.0 using 2N(His) at 1.89 Å, 1S(Cys) at 2.13 Å and 1N at 2.69 Å.

shells to the theory for the ox11.0 data does not lead to a significant improvement in the fit for this data.)

A simulation of the ox6.4 data that used two histidines, an S(Cys), and a sulfur at 3.0 Å (α = 0.024 Å<sup>2</sup>) instead of oxygen gave a fit with the parameters shown in Table 2. In order to accommodate the S at 3 Å, the Debye–Waller parameters for the second-shell carbon atoms of the imidazole rings have doubled to 0.014 Å<sup>2</sup>. This increase, along with the higher value (0.024 Å<sup>2</sup>) of σ<sup>2</sup> for S, does not argue in favor of this model.

*Reduced Stellacyanin*. The *k*<sup>3</sup>-weighted raw EXAFS spectra recorded from reduced Cu(I) stellacyanin at pH 6.4 (red6.4) and pH 11.0 (red11.0) shown in Figure 3 provide direct evidence that significant changes in the Cu environment take place upon reduction of the copper atom. In both of the reduced species, the amplitude of the EXAFS has decreased relative to the oxidized EXAFS. This is appreciated most clearly by comparing the Fourier transforms in Figure 3, where the amplitude of the first shell is smaller by about 30% in the reduced data. There is a similar decrease in the second- and third-shell Fourier transform amplitudes. A correlated decrease in the amplitudes of these three shells suggests that a change in histidine coordination occurs during reduction at both pH values. The two reduced species also exhibit different EXAFS profiles, at low *k* especially, and their Fourier transforms suggest some differences in their inner shell coordination. This is confirmed by detailed analysis, as set out below. Two possible schemes are considered. In scheme A, the number of histidine ligands was fixed at two and their distance and orientation were refined. In the second, scheme B, only one histidine was

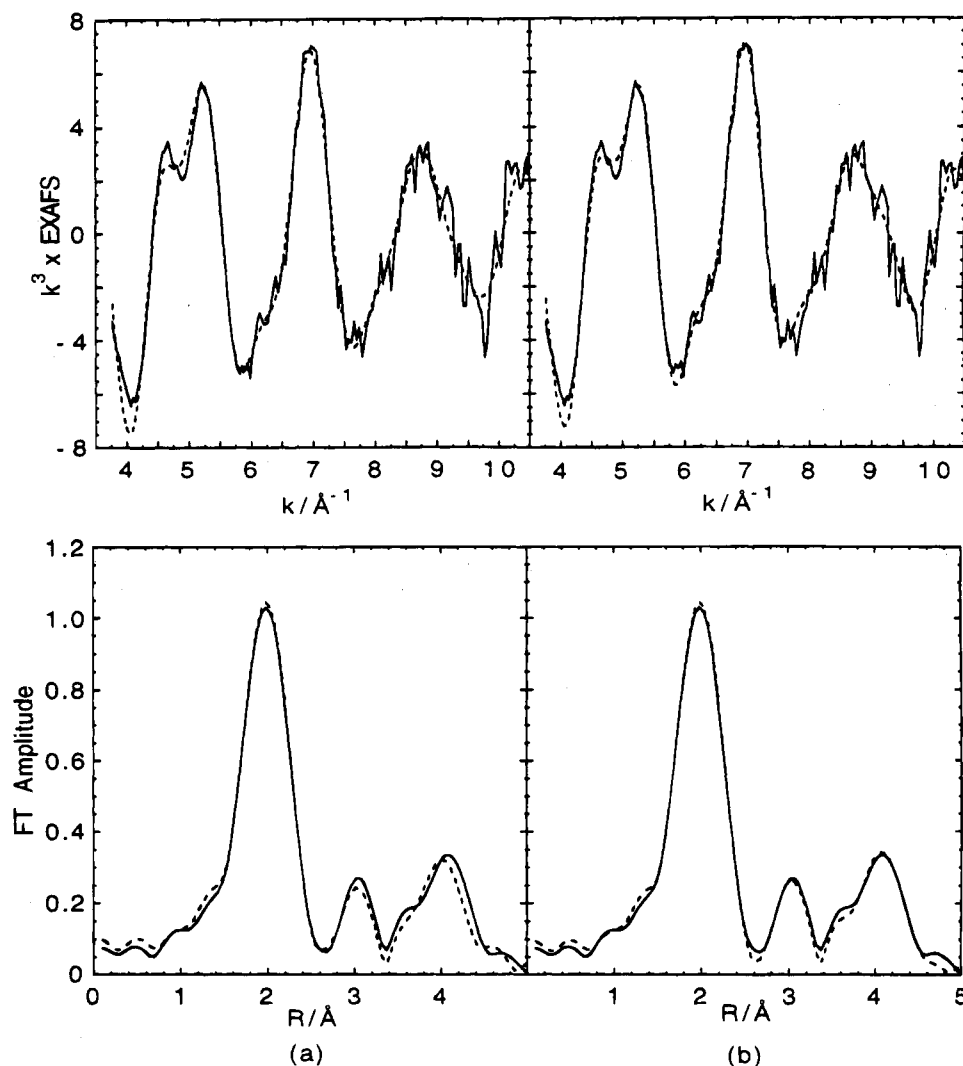


FIGURE 5: Simulation (dashed line) of oxidized stellacyanin EXAFS at pH 6.4 using (a) 2N(His) at 1.90 Å, 1S(Cys) at 2.14 Å and 1O at 2.70 Å. (b) Simulation (dashed line) with an additional sulfur backscatterer at 4.34 Å.

assumed to be coordinated in the inner shell of the reduced protein.

(1) *red6.4 EXAFS (Scheme A)*. In an initial constrained refinement of the EXAFS of reduced stellacyanin at pH 6.4, it was assumed that Cu was coordinated by two histidine ligands at the same distance, together with an S atom assumed to be from the cysteine ligand. This simulation resulted in a poor fit to the data, with FI = 0.79 and  $R = 32\%$ . Previous EXAFS studies of reduced stellacyanin at pH 7.2 (Feiters et al., 1988) found that an adequate simulation of the reduced data could be obtained for 2N atoms in the first shell, with  $\alpha_1 = 0.007 \text{ \AA}^2$ . It was also suggested that, in addition to the S(Cys), a second S atom was present at 2.66 Å. We have, therefore, tried to fit this model to our data by refining the two histidine and 1S(Cys) shells in the presence of a possible second S atom. A restrained refinement resulting from this gave an FI of 0.22 with a sulfur distance of 2.66 Å with a high Debye–Waller term ( $\alpha = 0.036 \text{ \AA}^2$ ). Such a high value for  $\alpha$  indicates that either a weaker backscattering ligand should be in this position or the ligand is highly disordered. However, the Debye–Waller parameters for the histidine shells in this model are inconsistent, with  $\alpha_1$  still very large ( $2\sigma^2 = 0.041 \text{ \AA}^2$ ) compared to  $\alpha(2,5)$  ( $2\sigma^2 = 0.010 \text{ \AA}^2$ ) and  $\alpha(3,4)$  ( $2\sigma^2 = 0.031 \text{ \AA}^2$ ). The large values of  $\alpha_1$  obtained for these refinements

suggests that the two histidine ligands are not coordinated to the copper at the same distance.

A second simulation therefore was carried out for a model with the two histidine ligands at different distances from the copper atom. Both histidines were included as separate units in multiple-scattering calculations. In this refinement, the number of parameters used was equal to the total number of parameters allowed in the restrained refinement procedure for the data range used ( $k = 3.5\text{--}10.2 \text{ \AA}^{-1}$ ). The refinement resulted in the simulation shown in Figure 6a and Table 3a. The improvement in FI by a factor of two demonstrates the inadequacy of the first-shell models, where the two histidines are forced to take up the same distance. The first shell is well simulated by four backscattering atoms: namely, 1N from histidine at 1.93 Å ( $\alpha = 0.001 \text{ \AA}^2$ ), 1S(Cys) at 2.17 Å ( $\alpha = 0.002 \text{ \AA}^2$ ), 1N from histidine at 2.16 Å ( $\alpha = 0.003 \text{ \AA}^2$ ), and 1N/O at 2.45 Å ( $\alpha = 0.004 \text{ \AA}^2$ ). The separation between the two histidines is consistent with what might be expected given the high value of  $\alpha_1$  when two histidines were forced to take up the same position.

*Scheme B*. In this case, only a single histidine was assumed to be present in the copper environment. The position of any additional low-Z ligand in the first shell was determined by a least-squares refinement involving the single histidine, the S(Cys), and a single N/O atom. The first shell

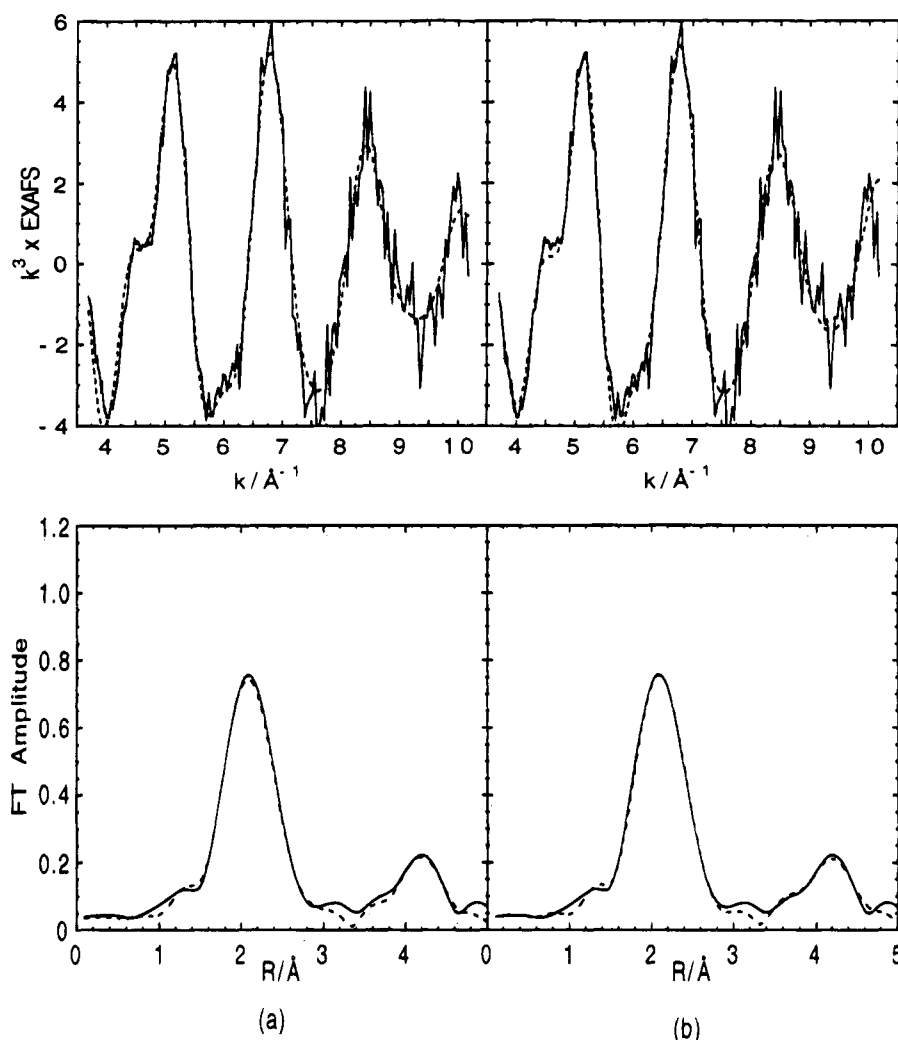


FIGURE 6: Simulation (dashed line) of reduced stellacyanin at pH 6.4 using (a) 1N(His) at 1.93 Å, 1N(His) at 2.16 Å, 1S(Cys) at 2.17 Å, and 1N at 2.45 Å or (b) 1N(His) at 1.92 Å, 1S(Cys) at 2.19 Å, 1N at 2.38 Å and 1S at 4.54 Å.

is well simulated by three backscattering atoms: 1N at 1.92 Å ( $\alpha = 0.002 \text{ Å}^2$ ), 1S(Cys) at 2.19 Å ( $\alpha = 0.002 \text{ Å}^2$ ), and 1N/O at 2.38 Å ( $\alpha = 0.011 \text{ Å}^2$ ). The 2.38 Å N/O contribution could represent the average distance of a histidine N at  $\sim 2.2$  Å and an N/O at  $\sim 2.5$  Å, and thus is similar to the model represented by scheme A. Inclusion of 1S at  $\sim 4.5$  Å ( $\alpha = 0.020 \text{ Å}^2$ ), consistent with the presence of this shell in the oxidized data at pH 6.4, results in FI = 0.10,  $R_d = 0.96\%$ , and  $R_e = 19.7\%$  (Figure 6b, Table 3b).

Attempts to include a second sulfur atom at  $\sim 3$  Å in both schemes were made (i) by replacing the long N/O scatterer at  $\sim 2.4$  Å by an S atom and refining (Cu–S = 2.61 Å,  $\alpha = 0.037 \text{ Å}^2$ ; FI = 0.62,  $R_e = 29\%$ ) and (ii) by including the S atom together with the long N/O atom and refining. In the latter case, the N/O contribution was clearly preferred and the S contribution was killed off completely.

(2) *red11.0* EXAFS. The EXAFS of reduced stellacyanin at pH 11.0 was also simulated (between  $k = 3.6$  and  $10.5 \text{ Å}^{-1}$ ) using models with two (scheme A) or one (scheme B) coordinated histidines. In scheme A (Table 4 and Figure 7 a), the EXAFS was accounted for by one histidine ligand at 1.90 Å ( $\alpha = 0.001 \text{ Å}^2$ ), one histidine at 2.12 Å ( $\alpha = 0.003 \text{ Å}^2$ ), and the S(Cys) at 2.16 Å ( $\alpha = 0.003 \text{ Å}^2$ ). In scheme B, a simulation was obtained with one histidine ligand at 1.92 Å ( $\alpha = 0.002 \text{ Å}^2$ ) and the S(Cys) at 2.16 Å ( $\alpha = 0.005 \text{ Å}^2$ ), as shown in Figure 7b and Table 4b. There was no

evidence in either scheme for a shell at  $\sim 2.4$  Å. In these simulations, weightings of 0.3 (EXAFS refinement) and 0.7 (distance refinement) have been used to obtain the optimum fit. This accounts for the much smaller values of FI, which, like  $R$ , depends upon the relative weighting used in the refinement, obtained for this sample compared to the simulations of the reduced protein at pH 6.4 (Binsted et al., 1992).  $R_e$  is independent of the weighting scheme used.

## DISCUSSION

**Oxidized Protein.** The basic coordination to the copper atom in oxidized stellacyanin at pH 6.4 is provided by two histidine ligands at 1.89 Å and one sulfur ligand from cysteine at 2.13 Å. The Cu–N(His) and Cu–S(Cys) distances are not significantly altered upon increasing the pH from 6.4 to 11.0. Both of these distances are shorter than the values obtained in previous EXAFS studies by Peisach et al. (1982) and Feiters et al. (1988), who agreed on a Cu–S(Cys) distance of 2.21 Å but found different Cu–N(His) distances of 1.96 and 1.93 Å, respectively. The shorter Cu–S(Cys) distance found in this study is close to those determined by others from the EXAFS of azurin and stellacyanin (Tullius et al., 1978; Tullius, 1979), of azurin and its methionine-121 mutants (Murphy et al., 1993), of amicyanin (Lommen et al., 1991), and of plastocyanin (Scott et al., 1982). It is also similar to the average value derived

Table 3: Parameters Used in the Simulations of Reduced Stellacyanin at pH 6.4<sup>a</sup>

(a) Scheme A: Constrained To Accommodate Two Histidines				
	<i>R</i> (Å)	2σ <sup>2</sup> (Å <sup>2</sup> )	φ (deg)	θ (deg)
1N(His)	1.93	0.001	0.0	90.0
1C(His)	2.85	0.002	25.4	93.3
1C(His)	3.03	0.002	343.0	94.6
1N(His)	4.02	0.004	14.4	97.3
1C(His)	4.13	0.004	354.8	97.8
1S(Cys)	2.17	0.002		
1N/O	2.45	0.002		
1N(His)	2.16	0.003	0.0	90.0
1C(His)	3.00	0.005	24.4	90.0
1C(His)	3.22	0.005	343.3	90.0
1N(His)	4.21	0.007	14.6	90.0
1C(His)	4.26	0.007	355.9	90.0
(b) Scheme B: One Histidine Removed				
	<i>R</i> (Å)	2σ <sup>2</sup> (Å <sup>2</sup> )	φ (deg)	θ (deg)
1N(His)	1.92	0.002	0.0	90.0
1C(His)	2.90	0.004	21.6	90.0
1C(His)	2.99	0.004	339.5	90.0
1N(His)	4.09	0.009	11.1	90.0
1C(His)	4.14	0.009	351.3	90.0
1S(Cys)	2.19	0.002		
1N/O	2.38	0.010		
1S	4.54	0.021		

<sup>a</sup> Scheme A: Constrained to accommodate two histidine ligands, FI = 0.10, *R*<sub>d</sub> = 0.90%, *R*<sub>e</sub> = 20.1%. Scheme B: One histidine ligand, FI = 0.10, *R*<sub>d</sub> = 0.96%, *R*<sub>e</sub> = 19.7%. The distance (*R*) and Debye–Waller term (2σ<sup>2</sup>) for each shell are shown together with the polar angles (φ, θ) of the imidazole ring atoms, as defined in Figure 1.

Table 4: Parameters Used in the Simulations of Reduced Stellacyanin at pH 11.0<sup>a</sup>

(a) Scheme A: Constrained To Accommodate Two Histidines				
	<i>R</i> (Å)	2σ <sup>2</sup> (Å <sup>2</sup> )	φ (deg)	θ (deg)
1N(His)	1.91	0.001	0.0	90.0
1C(His)	2.84	0.002	25.2	95.6
1C(His)	2.99	0.002	342.8	97.9
1N(His)	3.96	0.004	14.2	103.4
1C(His)	4.07	0.004	354.0	102.4
1S(Cys)	2.16	0.003		
1N(His)	2.12	0.003	0.0	90.0
1C(His)	3.01	0.005	23.8	92.1
1C(His)	3.17	0.005	342.4	93.1
1N(His)	4.19	0.010	13.6	94.9
1C(His)	4.22	0.010	354.7	95.3
(b) Scheme B: One Histidine Removed				
	<i>R</i> (Å)	2σ <sup>2</sup> (Å <sup>2</sup> )	φ (deg)	θ (deg)
1N(His)	1.92	0.002	0.0	90.0
1C(His)	2.87	0.004	23.5	92.1
1C(His)	3.02	0.004	341.5	93.2
1N(His)	4.06	0.009	11.8	95.1
1C(His)	4.14	0.009	352.3	95.4
1S(Cys)	2.16	0.005		

<sup>a</sup> Scheme A: Constrained to accommodate two histidine ligands, FI = 0.035, *R*<sub>d</sub> = 1.0%, *R*<sub>e</sub> = 18.3%. Scheme B: One histidine ligand, FI = 0.037, *R*<sub>d</sub> = 0.95%, *R*<sub>e</sub> = 19.9%. The distance (*R*) and Debye–Waller term (2σ<sup>2</sup>) for each shell are shown together with the polar angles (φ, θ) of the imidazole ring atoms, as defined in Figure 1. In this simulation, a weighting scheme of 0.3 (EXAFS refinement) and 0.7 (distance refinement) has been used to obtain the optimum fit. This accounts for the smaller FI range obtained for this sample compared to the reduced protein at pH 6.4 [see Binsted et al. 1993].

from six high-resolution crystal structures of type 1 copper proteins and is consistent with the predicted bond length based on resonant Raman studies of stellacyanin (Han et al., 1991). The different Cu–N(His) distances found by Peisach et al. (1982), Feiters et al. (1988), and this study may be

attributed to a number of factors, such as the use of plane wave EXAFS theory in the earlier study and the different central atom approximation for the *ab initio* phase shifts used by Feiters et al. (1988) compared to the present work. In addition, we have used a 13-element energy-dispersive solid-state detector in contrast to the scintillation counters used in the earlier work, which results in much improved data quality, largely due to better discrimination of the fluorescence signal from the scattered background.

In addition to the basic type 1 coordination at the copper site of the oxidized protein, EXAFS reveals the presence of an additional shell close to the copper atom. It is possible to fit either a low-Z atom at ~2.7 Å or a second sulfur atom at ~3 Å. However, the behavior of the Debye–Waller terms for the second shell of imidazole carbon atoms suggests a preference for a low-Z element. The presence of a second sulfur atom in the copper coordination sphere has been suggested by previous studies and also by analogy with the structures of other type 1 copper proteins where methionine is present (Dahlin et al., 1989; Bergman et al., 1977; McMillin & Morris, 1981; Ferris et al., 1978; Solomon et al., 1980). The presence of an additional oxygen or nitrogen ligand at the copper site has been suggested by ENDOR measurements and molecular modeling studies (Thomann et al., 1991; Fields et al., 1991).

One difficulty, observed for other type 1 copper proteins where a methionine sulfur is known to be present at about 2.9–3.1 Å, is that of distinguishing the contribution of this S atom from the contributions of the second-shell C atoms of the imidazole rings (Groeneveld et al., 1986; Tullius et al., 1978; Scott et al., 1982; Penner-Hahn et al., 1989; Lommen et al., 1991). The problem is complicated by the fact that multiple scattering of the photoelectron, involving the Cu–N1–C2/C5 atoms of the two imidazole rings, makes a contribution to the EXAFS in this region of the spectrum. In previous EXAFS studies on stellacyanin this contribution has not been taken into account. In this paper, as described earlier, we have included this contribution and we have also adopted a constrained–restrained fitting method, which forces the second (and third)-shell atoms of the imidazole ring to adopt a range of physically meaningful positions. Even this approach does not allow us to unambiguously determine whether or not S is present at ~3 Å—simulations with or without this S are still possible, as shown above—but it does provide a clearer means of assessing the likelihood of the fourth ligand being a sulfur ligand. For the oxidized data at pH 6.4, the simulation with the sulfur at 3.0 Å (FI = 0.081) clearly is inferior to the alternative simulation with oxygen at 2.70 Å (FI = 0.068). At pH 11.0 the fit with sulfur (FI = 0.079) is 10% worse than the fit with nitrogen (FI = 0.071). Also, there is no evidence in the EXAFS of reduced stellacyanin for the presence of a second S at ~3 Å or less. Completely unacceptable Debye–Waller terms arise if the S is included in the fits to the reduced data. The best simulations to the reduced data are found when the histidine ligands are allowed to coordinate at different distances, and in the pH 6.4 data a third low-Z ligand is also present. The simulations show a clear preference for the models with nitrogen or oxygen over the models with a second sulfur.

The origin of the O (or N) ligand at about 2.7 Å is not clear. We note that the model for the EXAFS data is consistent with the suggestion that the fourth ligand to copper is Gln97 (Guss et al., 1988; Fields et al., 1991). This idea



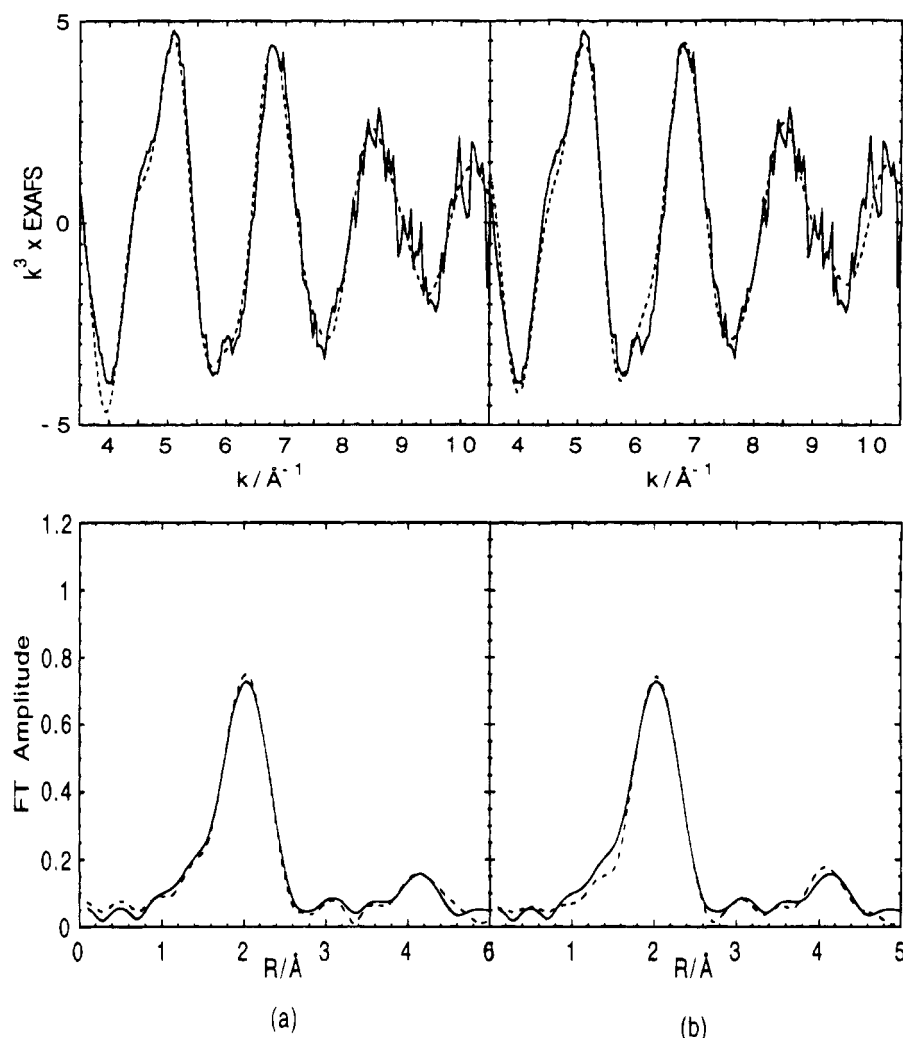


FIGURE 7: Simulation (dashed line) of reduced stellacyanin at pH 11.0 using (a) 1N(His) at 1.91 Å, 1N(His) at 2.12 Å, and 1S(Cys) at 2.16 Å or (b) 1N(His) at 1.92 Å and 1S(Cys) at 2.16 Å.

is supported by the pH dependent ENDOR studies of stellacyanin (Thomann et al., 1991), which indicate that an amide N from Gln97 provides a fourth ligand at high pH, where it is detected, and this shifts to an O at low pH, where the N is no longer detected by ENDOR. EXAFS is unable to distinguish between the N or O backscatterers, but a low-Z ligand is observed at both pH's, consistent with this proposal.

**The Contribution at ca. 4.3 Å.** The possibility that a contribution may arise from the presence of sulfur at 4.3 Å in the oxidized pH 6.4 data is an intriguing one. Firstly, there are the observations that the three cysteine residues in stellacyanin are close to each other and that there is a disulfide switch in apostellacyanin from Cys59–Cys93 to Cys87–Cys93 above pH 8.2 (Engeseth et al., 1984). Secondly, there is previous spectroscopic data suggesting that the disulfide bridge is close to the copper site (Ferris et al., 1978; McMillin & Morris, 1981; Dahlin et al., 1989). This model gets support from the present observation that a significant backscattering contribution at ~4.3 Å is best accounted for by an S atom with a low Debye–Waller term of only 0.010 Å<sup>2</sup> at pH 6.4. When the pH is raised to 11.0, there is no longer any requirement for this shell. We note that in previous EXAFS studies on a number of type 1 copper proteins, in which curved-wave multiple-scattering theory has been employed, it has not been necessary to include such a contribution. The backscattering in this range has been

accounted for by single and multiple scattering from the histidine ring atoms alone. This has been the case in the EXAFS analyses of azurin, plastocyanin, and rusticyanin (Murphy et al., 1991, 1993), each of which has the same basic copper coordination environment.

**Reduced Protein.** The EXAFS of the Cu(I) protein reveals that major changes in coordination occur upon reduction. Two alternative structures for the reduced copper site at each pH have emerged with detailed analysis. One of these, scheme A, is shown in Figure 8. When the copper site is forced to incorporate two histidines, it is four-coordinate at pH 6.4 and three-coordinate at pH 11.0, results that agree with the interpretation of the XANES data given earlier. In both cases, one of the histidine ligands is moved away from copper by ca. 0.2 Å, accompanied by small changes in the positions of the second histidine and the S(Cys). A similar splitting of the histidine coordination has been observed in the high-pH Cu(I) site of amicyanin from *Thiobacillus versutus* (Lommen et al., 1991). These changes in the ligand coordination are observed at both pH values, but they are more pronounced at pH 11.0, as may be seen by comparing the distances and angular parameters in Tables 3a and 4a. At pH 6.4, one of the histidine imidazole rings is tilted out of the x,y plane by 8°; at pH 11.0, both imidazole rings are out of the plane, by 12° and 5° respectively. The rotations were necessary to accommodate both histidines in the fit.

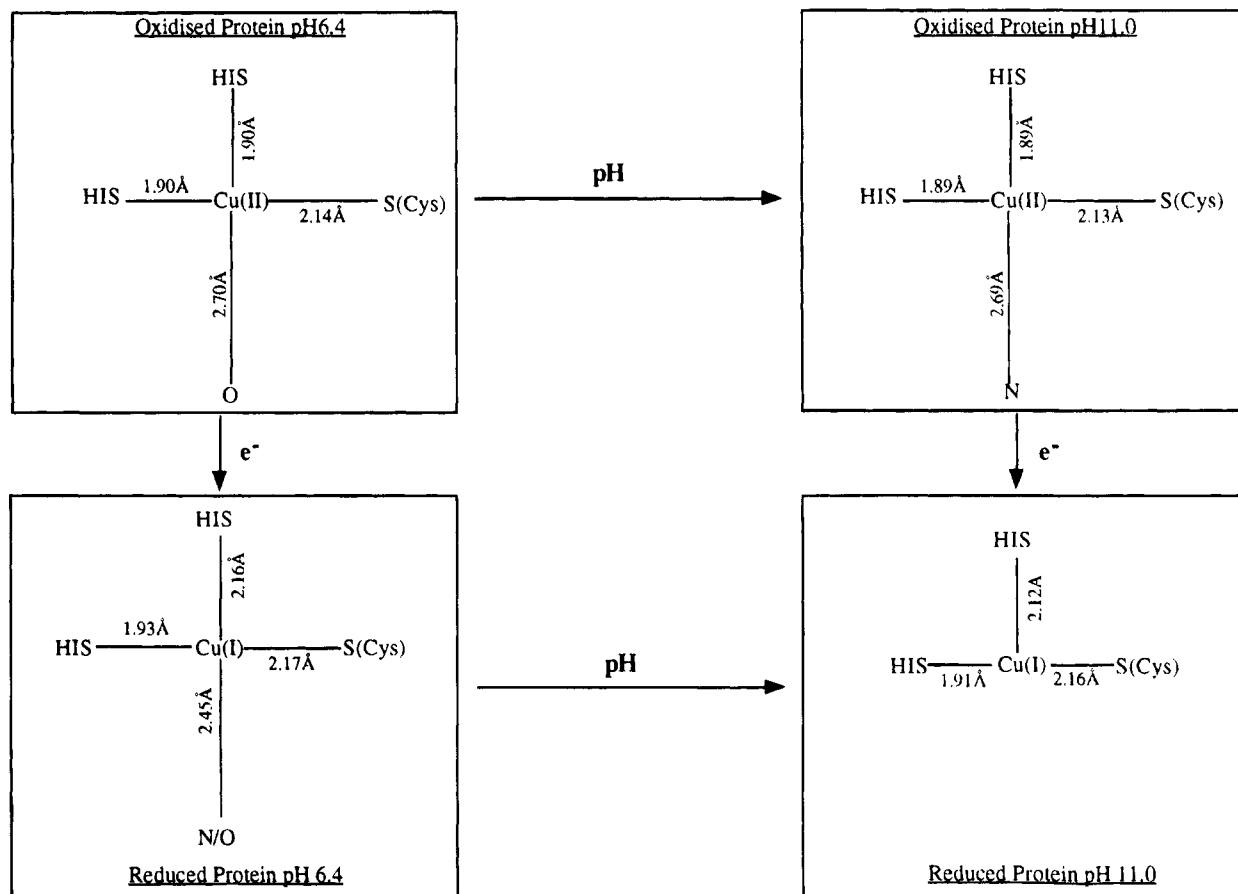


FIGURE 8: Copper site of stellacyanin: models based on scheme A for the Cu coordination as suggested by the EXAFS analysis. The changes associated with variations in pH and oxidation state are shown. Data for the reduced protein are also consistent with a larger movement of one histidine from the copper atom (scheme B, see text).

Reduction of the copper site at pH 11.0 also results in the loss of the fourth low-Z ligand. The loss of a ligand at 2.4 Å might be due to a conformational change (which is also evident from the EXAFS data) at higher pH values. This change could depend on the titration of Lys91, which is the nearest neighbor to His92, one of the histidine ligands to copper. The pH dependence of the optical absorption and EPR spectra in oxidized stellacyanin could also be due to titration of this Lys. A similar suggestion was made by Romero et al. (1993), who observed no pH dependence in their mutant Gln121, where this residue is replaced by a glycine. Amino acid sequence comparisons of a number of type 1 copper proteins reveal that glycine is found in the equivalent position in the sequence in several other species, including CBP, but lysine is present at this position only in stellacyanin.

When only a single histidine is assumed to be coordinated, scheme B, the copper site at pH 6.4 is three-coordinate, and at pH 11.0 it is only two-coordinate. A two-coordinate site in which one of the histidine ligands is displaced by about 1 Å from the copper upon reduction has been reported for the crystal structure of the Gln121 mutant of *Alcaligenes denitrificans* azurin (Romero et al., 1993). Interestingly, the Cu(II) site of this protein is proposed as a model for stellacyanin. A two-coordinate Cu(I) site disagrees with the coordination based on the XANES of Cu(I) systems, which suggests a copper site that is likely to be three-coordinate or more (Kau et al., 1987; Blackburn et al., 1989, 1992).

It is clear that, in reduced stellacyanin, one of the histidine ligands moves away from the copper atom: in scheme A

by ~0.2 Å and in scheme B by as much as 1 Å. A small change in the copper coordination geometry between Cu(II) and Cu(I) is likely to be more favorable for electron transfer, which suggests a preference for scheme A. We note that the change in the reduced copper site as a function of pH for stellacyanin is the reverse of the pH dependent behavior of *Populus nigra* plastocyanin. Crystallographic studies on *P. nigra* plastocyanin (Guss et al., 1986) show that, at low pH (3.8), one of the histidine ligands (His87) is ca. 3 Å from the Cu atom. In this state, the plastocyanin copper site has trigonal-planar geometry and the protein is redox inactive. Stellacyanin maintains its redox activity between pH 6.4 and 11.0, which argues in favor of two histidines being coordinated in the reduced protein at both pH's.

**Comparison with Azurin Mutants.** We have recently reported the results of some spectroscopic and XAFS studies on a number of methionine-121 mutants of azurin from *Pseudomonas aeruginosa* (Murphy et al., 1993). Some of the relevant aspects are worth discussing here. The EPR and optical data of Asp121 showed a marked change with pH. The EPR spectrum was a typical axial type 1 copper spectrum at pH 5.0, but it became rhombic at pH 8.0 and similar to the EPR data for stellacyanin shown in Figure 2. The optical spectrum for Asp121 showed a corresponding pH dependence, with the data at pH 8.0 being similar to the stellacyanin spectrum in Figure 2. The EXAFS data of the Cu(II) form of the mutant at both pH 5.0 and pH 8.0 revealed the presence of two histidine ligands at ~1.93 Å, an S(Cys) ligand at ~2.15 Å, and a fourth ligand (oxygen or nitrogen) at ~2.26 Å. The structural change that occurred when the

pH was varied from 8.0 to 5.0 was the loss of a low-Z ligand (from aspartic acid or water) at  $\sim 2.9$  Å in the low-pH data. Thus, in the Asp121 mutant of azurin, the distant axial interaction of a low-Z ligand at the copper site was suggested to account for the observed spectroscopic behavior with pH. A second mutant was End121, where the optical and EPR data were both similar to the data for stellacyanin shown in Figure 2, but did not show pH dependence. The EXAFS analysis of End121 showed a similar coordination environment to the Asp121 mutant at pH 8.0, including a short 2.26 Å O shell and the presence of a distant oxygen/nitrogen at 2.83 Å. Also, the reduction potential of the End121 mutant (205 mV, pH 7.1) was almost as low as that for stellacyanin (184 mV, pH 7.0). The reduction potential of the Asp121 mutant was higher (287 mV, pH 8.0). In view of these observations, it may have been tempting to conclude that the copper site of the End121 mutant of azurin is a reasonable model for stellacyanin. However, structural information on the copper coordination in stellacyanin, obtained here using EXAFS, shows that this is not the case. In particular, stellacyanin does not show the  $\sim 2.26$  Å oxygen observed in both the End121 and Asp121 mutants. Furthermore, the lack of any pH dependence for the spectroscopic properties of the End121 mutant clearly indicates its inadequacy as a model for the Cu site of stellacyanin.

Our recent work on another azurin mutant, Glu121 from *Pseudomonas aeruginosa* (Strange et al., manuscript in preparation), shows that its copper coordination at pH 4.0 is identical to that for End121, except that the oxygen shell at 2.26 Å is missing. In an earlier study, we proposed that this shell could be identified as an oxygen either from a water ligand or from the carbonyl of the Gly45 ligand. The absence of this shell from the Glu121 data would be consistent with this oxygen arising from a water molecule, present in End121 and Asp121 but excluded from the Glu121 Cu site due to the bulk of the glutamate side chain. The inner coordination sphere of Glu121 at pH 4.0 is similar to that of stellacyanin (Strange et al., unpublished results), suggesting that the fourth ligand in stellacyanin is of a similar nature.

The Gln121 mutant of azurin from *Alcaligenes denitrificans* has recently been proposed as a model for the Cu(II) site of stellacyanin, primarily because of the similarity of its EPR and optical spectra (Romero et al., 1993). A 1.9 Å resolution X-ray structure of this mutant has been obtained from crystals grown at pH 5.2. The data show an averaged Cu(II) coordination consisting of the two histidines at 1.93 Å and 2.05 Å, and the cysteine at 2.12 Å. In addition, there is an oxygen from the Gln121 residue at 2.26 Å. The present work does not show the presence of a short ( $\sim 2.26$  Å) low-Z ligand. Also, the Gln121 mutant of *Alcaligenes denitrificans* azurin, like the End121 mutant of *Pseudomonas aeruginosa* azurin (Murphy et al., 1993), does not exhibit the type of pH dependence in its spectroscopic properties that is shown by stellacyanin. In addition, the reduction potential for Gln121 (263 mV) is significantly higher than that for stellacyanin (184 mV).

## CONCLUSIONS

Even though the exact nature of the fourth ligand in oxidized stellacyanin has not been identified, the data are most consistent with an oxygen (or nitrogen)-donating ligand.

The fourth ligand is not present in the inner coordination sphere, but makes a more distant interaction at 2.7 Å from the copper atom. The spectroscopic similarity between stellacyanin and the End121 and Asp121 mutants of azurin suggests that this distant interaction has a significant role to play in determining the optical and magnetic properties of the copper site. The distinct structural differences between the azurin mutants and stellacyanin, which are revealed by the XAFS data, show that these mutant proteins are not adequate models for the copper site of stellacyanin. Data for the reduced protein show that one of the histidine ligands is displaced from the copper site by at least 0.2 Å and that there is a loss of one ligand at high pH. This behavior is opposite that found for plastocyanin, where one of the histidine ligands moves away from the Cu atom by  $\sim 1$  Å at low pH, consistent with its redox inactive state at this pH.

## ACKNOWLEDGMENT

We thank the U.K.'s Science and Engineering Research Council and the Swedish Research Council for their research support. We also thank our colleagues at the two institutes for their help and support.

## REFERENCES

- Adman, E. T. (1985) *Topics in Molecular and Structural Biology: Metalloproteins* (Harrison, P., Ed.) Vol. 1, pp 1–46, Macmillan, New York.
- Adman, E. T., & Jensen, L. H. (1981) *Isr. J. Chem.* 21, 8.
- Baker, E. N. (1988) *J. Mol. Biol.* 203, 1071.
- Bergman, C., Gandvik, E.-K., Nyman, P. O., & Strid, L. (1977) *Biochem. Biophys. Res. Commun.* 77, 1052.
- Binsted, N., Gurman, S. J., Campbell, J. W., & Stephenson, P. (1991) *SERC Daresbury Laboratory Program EXCURVE*.
- Binsted, N., Strange, R. W., & Hasnain, S. S. (1992) *Biochemistry* 31, 12117.
- Blackburn, N. J., Strange, R. W., McFadden, L. M., & Hasnain, S. S. (1987) *J. Am. Chem. Soc.* 109, 7162.
- Blackburn, N. J., Strange, R. W., Farooq, A., Haka, M. S., & Karlin, K. D. (1988) *J. Am. Chem. Soc.* 110, 4263.
- Blackburn, N. J., Strange, R. W., Reedijk, J., Volbeda, A., Farooq, A., Karlin, K. D., & Zubieta, J. (1989) *Inorg. Chem.* 28, 1349.
- Blackburn, N. J., Strange, R. W., Carr, R. T., & Benkovic, S. J. (1992) *Biochemistry* 31, 5298–5303.
- Blair, D. F., Campbell, G. W., Schoonover, J. R., Chan, S. I., Gray, H. B., Malmström, B. G., Pecht, I., Swanson, B. I., Woodruff, W. H., Cho, W. K., English, A. M., Fry, H. A., Lum, V., & Norton, K. A. (1985) *J. Am. Chem. Soc.* 107, 5755.
- Dahlin, S., Reinhammar, B., & Ångström, J. (1989) *Biochemistry* 28, 7224.
- Engeseth, H. R., Hermodson, M. A., & McMillan, D. R. (1984) *FEBS* 171 (2), 257.
- Feiters, M. C., Dahlin, S., & Reinhammar, B. (1988) *Biochim. Biophys. Acta* 955, 250.
- Ferris, N. S., Woodruff, W. H., Rorabacher, D. B., Jones, T. E., & Ochrymowycs, L. A. (1978) *J. Am. Chem. Soc.* 100, 5939.
- Fields, B. A., Guss, J. M., & Freeman, H. C. (1991) *J. Mol. Biol.* 222, 1053.
- Gray, H. B., & Malmström, B. G. (1983) *Comments Inorg. Chem.* 2, 203.
- Groeneveld, C. M., Feiters, M. C., Hasnain, S. S., Van Rijn, J., Reedijk, J., & Canters, G. W. (1986) *Biochim. Biophys. Acta* 873, 214.

- Gurman, S. J., Binsted, N., & Ross, I. (1984) *J. Phys. C* **C17**, 143.
- Gurman, S. J., Binsted, N., & Ross, I. (1986) *J. Phys. C* **C19**, 1845.
- Guss, J. M., & Freeman, H. C. (1983) *J. Mol. Biol.* **169**, 521.
- Guss, J. M., Harrowell, P. R., Murata, M., Norris, V. A., & Freeman, H. C. (1986) *J. Mol. Biol.* **192**, 361.
- Guss, J. M., Merritt, E. A., Phizackerley, R. P., Hedman, B., Murata, M., Hodgson, K. O., & Freeman, H. C. (1988) *Science* **241**, 806.
- Han, J., Adman, E. T., Beppu, T., Codd, R., Freeman, H. C., Huq, L., Loehr, T. M., & Sanders-Loehr, J. (1991) *Biochemistry* **30**, 10904.
- Hasnain, S. S., & Strange, R. W. (1990) *Biophysics and Synchrotron Radiation*. (Hasnain, S. S., Ed.) p 104, Ellis Horwood Ltd., Chichester, U.K.
- Hill, H. A. O., & Lee, W. K. (1979) *J. Inorg. Biochem.* **11**, 101.
- Karlsson, B. G., Nordling, M., Pascher, T., Tsai, L.-C., Sjölin, L., & Lundberg, L. G. (1991) *Protein Eng.* **4** (3), 343.
- Kau, L., Spira-Solomon, D., Penner-Hahn, J. E., Hodgson, K. O., & Solomon, E. I. (1987) *J. Am. Chem. Soc.* **109**, 6433.
- Lommen, A., Pandya, K. I., Koningsberger, D. C., & Canters, G. W. (1991) *Biochim. Biophys. Acta* **1076**, 439.
- Malmström, B. G., Reinhammar, B., & Vänngård, T. (1970) *Biochim. Biophys. Acta* **205**, 48.
- McMillin, D. R., & Morris, M. C. (1981) *Proc. Natl. Acad. Sci. U.S.A.* **78**, 6567.
- Morrell, C., Baines, J. T. M., Campbell, J. W., Diakun, G. P., Dobson, B. R., Greaves, G. N., & Hasnain, S. S. (1989) EXAFS Users' Manual. Daresbury Laboratory, Warrington, UK.
- Murphy, L. M., Hasnain, S. S., Strange, R. W., Harvey, I., & Ingledew, W. J. (1991) *X-Ray Absorption Fine Structure* (Hasnain, S. S., Ed.), pp 152–155, Ellis Horwood Ltd., Chichester, U.K.
- Murphy, L. M., Strange, R. W., Karlsson, G., Lundberg, L., Pascher, T., Reinhammar, B., & Hasnain, S. S. (1993) *Biochemistry* **32**, 1965.
- Murphy, L. M., Strange, R. W., Karlsson, G., Lundberg, L., Reinhammar, B., & Hasnain, S. S. (1994) *Biochemistry* (in press).
- Norris, G. E., Anderson, B. F., & Baker, E. N. (1986) *J. Am. Chem. Soc.* **108**, 2784.
- Orpen, A. G., Brammer, L., Allen, F. H., Kennard, O., Watson, D. G., & Taylor, R. (1989) *J. Chem. Soc., Dalton Trans. (Suppl)*, S1.
- Peisach, J., Powers, L., Blumberg, W. E., & Chance, B. (1982) *Biophys. J.* **38**, 277.
- Penner-Hahn, J. E., Murata, M., Hodgson, K. O., & Freeman, H. C. (1989) *Inorg. Chem.* **28**, 1826.
- Reinhammar, B. (1970) *Biochim. Biophys. Acta* **205**, 35.
- Reinhammar, B. (1979) *Advances in Inorganic Biochemistry* (Eichhorn, G. L., et al., Eds.), p 92, Elsevier/North Holland, New York.
- Roberts, J. E., Cline, J. F., Lum, V., Freeman, H., Gray, H. B., Piesach, J., Reinhammar, B., & Hoffman, B. F. (1984) *J. Am. Chem. Soc.* **106**, 5324.
- Romero, A., Hoitink, C. W. G., Nar, H., Huber, R., Messerschmidt, A., & Canters, G. W. (1993) *J. Mol. Biol.* **229**, 1007–1021.
- Scott, R. A., Hahn, J. E., Doniach, S., Freeman, H. C., & Hodgson, K. O. (1982) *J. Am. Chem. Soc.* **104**, 5364.
- Solomon, E. I., Hare, J. W., Dooley, D. M., Dawson, J. H., Stephens, P. J., & Gray, H. B. (1980) *J. Am. Chem. Soc.* **102**, 168.
- Strange, R. W., Blackburn, N. J., Knowles, P. F., & Hasnain, S. S. (1987) *J. Am. Chem. Soc.* **109**, 7157.
- Thomann, H., Bernado, M., Baldwin, M. J., Lowery, M. D., & Solomon, E. I. (1991) *J. Am. Chem. Soc.* **113**, 5911.
- Tullius, T. D. (1979) Ph.D. Thesis, Stanford University, Palo Alto, CA.
- Tullius, T. D., Frank, P., & Hodgson, K. O. (1978) *Proc. Natl. Acad. Sci. U.S.A.* **75** (9), 4069.
- Wherland, S., Farver, O., & Pecht, I. (1988) *J. Mol. Biol.* **204**, 407.

BI9416871